

# The gamma-ray arc-minute imaging system (GRATIS): mechanical design and expected performance

Michael Seiffert  
Philip Lubin

Department of Physics  
University of California, Santa Barbara  
Santa Barbara, California 93106

Charles J. Hailey  
Klaus P. Ziock

Laboratory for Experimental Astrophysics  
Lawrence Livermore National Laboratory  
Livermore, California 94550

Fiona A. Harrison  
Steven M. Kahn

Department of Physics and Space Sciences Laboratory  
University of California, Berkeley  
Berkeley, California 94720

## ABSTRACT

We are constructing a balloon experiment, GRATIS, which will perform the first arcminute imaging of cosmic sources in the 30 - 200 keV energy band. Observations conducted with GRATIS can provide data relevant to several key problems in high energy astrophysics including the physical processes responsible for the high energy tail observed in the soft gamma-ray spectra of clusters of galaxies and the origin of both the diffuse and point source components of the gamma-ray emission from the Galactic Center. This paper discusses the scientific motivations in more detail, outlines the experiment, discusses several aspects of the design and construction of hardware components, gives an overview of the stabilized platform, and shows the expected performance and sensitivity.

## 1. INTRODUCTION

Within the discipline of gamma-ray astronomy, primary emphasis in recent years has been devoted to the development of instrumentation with high resolution spectroscopic capabilities as opposed to high resolution imaging capabilities. There are several reasons that can be offered for this relative prioritization. (1) First, many of the scientific programs which have been identified are concentrated in the area of nuclear astrophysics, where detection of narrow emission lines with good sensitivity is crucial. The scientific importance of high resolution imaging has received far less attention. Usually, the only motivation cited involves point-source location and identification, especially in crowded fields. (2) Second, high resolution imaging systems are difficult to implement at gamma-ray energies. Grazing incidence optics are no longer effective, and coded aperture mask arrangements with fine pixel sizes are non-trivial to fabricate. (3) Finally, the

development of imaging photodetectors with the required spatial resolution is technical challenging.

The first soft gamma-ray astrophysics experiment to emphasize imaging explicitly is EXITE<sup>2,3,4</sup>, a two meter focal length coded aperture system with a large area gamma-ray image intensifier in the focal plane. EXITE has an angular resolution of  $\sim 20$  arcminutes and has been successfully flown from a balloon-borne stabilized platform. As an evolution of this concept, we are constructing a balloon experiment, the Gamma-Ray Arc-minute Telescope Imaging System (GRATIS), which has arcminute angular resolution in the same energy band. Arcminute angular resolution gives us the potential to map out truly diffuse gamma-ray emission from extended objects. As we discuss below, this can provide a new and unique tool for investigating physical processes in many cosmic sources.

In this paper, we discuss our scientific objectives and summarize current progress in the design and construction of the GRATIS payload. In Section 4, we discuss the prototype collimators and masks which have been fabricated for the coded aperture imaging system. The construction of the balloon stabilized platform is outlined in Section 5. Finally, we present in section 6 results from our Monte Carlo sensitivity calculation and discuss the expected performance of the GRATIS instrument.

## 2. SCIENTIFIC MOTIVATION

There are a number of diverse scientific investigations which can profitably exploit the unique imaging potential of the GRATIS experiment. Below, we concentrate specifically on two areas which look especially promising.

### *Clusters of Galaxies:*

The spectra of the brightest clusters of galaxies exhibit distinct nonthermal tails which extend up to several hundred keV. These emission components are swamped at soft X-ray energies by thermal bremsstrahlung radiation from hot ( $10^8$  K) gas gravitationally bound in the overall cluster potential. Only at energies greater than 20 keV is investigation of the origin of the energetic component feasible. Possible sources of this emission are 1) active galactic nuclei associated with one or more member galaxies, and 2) the upscattering of microwave background photons by the relativistic electrons which permeate the intracluster medium. Determination of the origin of this emission would make a key contribution to several aspects of cluster astrophysics. In particular, measurement of the intensity of gamma-ray emission produced by upscattering of the microwave background photons would yield key constraints on the relativistic electron and magnetic field distributions within the intracluster medium. The radio emission from halos in these clusters is well established to be synchrotron radiation from relativistic electrons spiraling in the intracluster magnetic field. The radio flux depends on the product of the relativistic electron density and the magnetic field strength. The intensity of gamma-ray inverse Compton emission depends on the relativistic particle density alone. The detection of this emission would thus serve to establish both the electron density and the magnetic field strength, and would be the first positive determination of these quantities. Even the failure to detect the inverse Compton flux would place useful lower limits on the magnetic field strength. Among our principal targets are clusters from which gamma-ray emission has been positively detected. These include Perseus, M87 and the Virgo cluster, Coma, and Abell 2142. Additional candidate targets include clusters for which evidence of non-thermal excess exist, and which also exhibit extended radio emission (e.g. A1367 and A2319).

### *The Galactic Center*

Previous imaging surveys of the Galactic Center with resolution comparable to GRATIS have been conducted in the 1-15 keV band with Spartan I<sup>12</sup> and in the 3-30 keV band with an experiment on SPACELAB.<sup>13</sup> A balloon observation in the 30 keV - 5 MeV band<sup>14</sup> also detected significant flux, but had angular resolution of only 1°. These surveys have shown that the gamma-ray emission from the Galactic Center (GC) is comprised of both truly diffuse and multiple point source components.

Skinner et. al.<sup>13</sup> detected very strong diffuse emission at energies up to 30 keV emanating directly from the GC. The emission extends about 1° from the galactic nucleus and drops off sharply at a radius of about 72 arcminutes. With the sensitivity expected for GRATIS the diffuse component discovered by Skinner et. al. will be directly mapped with arcminute resolution in the energy band above 30 keV. This is of crucial importance in constraining proposed models for this emission.

Skinner et. al. also detected 9 point source emitters in the 3-30 keV band. Cook et. al.<sup>14</sup> detected one source in the 30 keV-3 MeV band consistent with the position of 1E1740.7-2942. With our calculated sensitivity and the measured source spectral properties, GRATIS will detect all of the sources discovered by Skinner et. al. if the power law spectra determined by their experiment extend out to higher energies. Thus GRATIS will provide a very powerful tool for clarifying the nature of these point source components.

## **3. OVERVIEW OF THE SYSTEM**

A schematic diagram of the telescope and gondola package appears in Figure 1. The major components of the telescope are the coded aperture mask plane, detector compartment, and telescope frame. The gondola frame supports the telescope and electronics compartment as well as houses the reaction wheel, elevation drive, and coarse azimuth control.

The gamma-ray telescope consists of approximately 36 individual, co-aligned, smaller telescopes. Each of these is a one-dimensional imaging telescope consisting of a coded aperture mask and a collimator above a CsI crystal scintillator coupled to a position sensitive (in two dimensions) photomultiplier tube. The 36 small telescopes are all rotated with respect to one another and a two-dimensional image is reconstructed from the set of rotated one-dimensional images using the Maximum Entropy Method. A diagram of one of the small 1-D telescopes appears in Figure 2. More details of the imaging scheme can be found in ref. 6.

## **4. HARDWARE COMPONENTS**

### **4.1 Telescope frame**

Translating the high spatial resolution of the detector plane into high angular resolution requires the telescope to be as long as possible. The telescope frame must also be rigid. In order to preserve the imaging scheme the lateral displacement of the coded aperture mask with respect to the detector plane must be less than a detector pixel. In order to meet these requirements, we have designed an aluminum frame that is approximately 1 meter square by 4 meters long. A preliminary engineering analysis has shown that there will be approximately 0.4 mm flexure displacement between the mask and detector planes.

### **4.2 Detector shielding**

We will use a combination of active shields for charged particle rejection and passive shields to reduce atmospheric gamma radiation and x-ray fluorescence. The active shield is a standard plastic scintillator (NE 110) coupled to phototubes. The passive shield is a graded Z shield and consists of a 3 mm outer layer of lead, a middle layer of 1 mm of tin, and an inner layer of 1 mm copper. The outer layer essentially stops all gamma-rays in our energy range and increasing the thickness only down-scatters more gammas from higher energies.

### 4.3 Collimators

One must collimate each detector pixel to one cycle of the mask pattern in order to prevent artifacts in the reconstructed image. This means long thin foils in front of the detector plane that are flat compared to the pixel dimension. Our design consists of commercially available graded Z laminate foils that are rolled flat to within 0.025 mm. The foils are then sandwiched between aluminum spacers and glued together inside an aluminum frame. The laminate consists of 5 layers: .050 mm Cu - .025 mm Sn - .025 mm Pb - .025 mm Sn - .050 mm Cu.

### 4.4 Coded aperture mask

Because our telescope consists of an array of smaller individual 1-D telescopes, we only need an array of 1-D coded aperture masks which are more simply fabricated than a 2-D mask. Each 1-D mask corresponds to an individual collimator and phototube assembly and is co-aligned with it. The small 1-D masks will be assembled from small bars of tantalum.

## 5. STABILIZED PLATFORM

Our goal in building the stabilized platform is to achieve 0.3 arcminute precision tracking in azimuth and elevation. The design for the system is similar to the UCSB group's recent stabilized platform for a cosmic background radiation (CMBR) anisotropy experiment.<sup>15</sup> This gondola achieved tracking with 0.3 arcminutes rms error in azimuth and 2 arcminutes rms error in elevation. The elevation tracking during one segment of a balloon flight from Palestine, Tx is shown in Figure 3a. The desired elevation (straight line) is shown along with the achieved elevation. The stepped nature of the elevation is caused by the finite resolution of the ballscrew linear actuator, which is due to gear backlash and ball screw play. We expect much better elevation stability from the torque motor-driven design of the GRATIS gondola, which does not suffer from these finite resolution problems. The dominant source of error in azimuth pointing in the CMBR experiment was overshoot and oscillations caused by chopping between three different points on the sky (Figure 3b). For the GRATIS system we point continuously on-source, and are limited in pointing precision only by the precision of the position sensing

### 5.1 Stabilized platform position sensing

We have two primary systems for position sensing: an inertial guidance system and a star camera. Our gyro-based inertial guidance system provides three-axis pointing information with approximately 20 arcsecond precision. This is a true inertial guidance system with gyros, accelerometers, and an integral navigational processor. Once aligned and initialized, the system is capable of determining pointing direction, angular rates, latitude, longitude, and surface velocity. The gyros have high relative pointing precision, but a slow drift component degrades their absolute accuracy. To correct drift, we will use a microchannel plate intensified CCD camera with an 8 inch diameter optical telescope as a star camera. We will monitor the video image at the ground station, allowing us to correct for gyro drifts and maintain their absolute accuracy. We are experimenting with another CCD system that will provide a direct closed-loop star tracking

servo link. With magnification in the telescope, this will give even higher pointing stability. We are also developing our daytime star tracking ability with a small format IR InSb CCD array.

## 5.2 Stabilized platform pointing control

The pointing control of the gamma-ray telescope is an azimuth-elevation system controlled by an on-board 80186 microprocessor based computer system. The elevation of the telescope is driven by 50 ft-lb samarium-cobalt torque motor about the telescope's center of mass. The entire gondola slews and tracks in azimuth to provide correct pointing for the telescope. The gondola has a coarse adjustment through a 20 ft-lb torque motor that torques directly against the cables to the balloon. This torque motor is part of a zero static friction bearing assembly that decouples the balloon from the gondola during fine azimuth adjustment and tracking. The fine adjustment is provided by a 200 lb, 36 inch diameter reaction wheel driven by a 46 ft-lb torque motor and mounted to the base of the gondola frame. All of the torque motors are controlled by pulse width modulated power amplifiers coordinated by the on-board computer.

## 5.3 Control software

We have developed two software servo control systems.<sup>16</sup> The first is proportional-integral-derivative (PID) control in which the analog output to the servo motors is the sum of three components: a term proportional to the error angle, a term proportional to the time derivative of the error angle, and a term proportional to the time integral of the error angle. The constants of proportionality are determined by extensive computer simulation and ground testing. The second available control system is the model referenced adaptive control (MRAC) and is considerably more complex. The MRAC system constantly monitors the system response and adjusts the software gains to the servo motor controllers to optimize stability. This is an important capability in stabilized platforms with large changing moments of inertia accompanying telescope elevation changes or ballast dropping.

## 6. EXPECTED PERFORMANCE

Table 1 lists the performance specifications of GRATIS system. The angular resolution is fixed by the length of the telescope and the spatial resolution of the detector plane. The 9% energy resolution at 122 keV is typical of sodium activated CsI crystal scintillators. We have quoted  $1.5^\circ$  as the nominal field of view, but we have considerable flexibility in choosing the field of view to meet our scientific objectives.  $346 \text{ cm}^2$  is the effective area of the detector at 122 keV after including the obscuration of the detector plane by the coded aperture masks and collimators and the detector efficiency. The geometrical detector area is  $800 \text{ cm}^2$ . Our ability to localize a point source depends on the strength of the source. For a 10 sigma detection, our theoretical source localization is  $< 0.2$  arcminutes.

## 7. EXPECTED SENSITIVITY

Figure 4 is a plot of a Monte Carlo calculation of the sensitivity of GRATIS. The Monte-Carlo includes all the important sources of background. Estimates of background obtained from the Monte-Carlo are used to optimize the thicknesses of graded Z collimators and shields and to determine the background absorbed in the crystal volume. The ability to detect the sources is somewhat distinct from our ability to image diffuse emission, which depends on the spatial extent of the emitting region and, in the case of clusters of galaxies, the ratio of point source to diffuse emission. Coupling results from the Monte-Carlo for sources of known strength to image reconstruction programs allow us to estimate the sensitivity of the experiment as a function of the

extent of the source emission region and the ratio of point source to diffuse emission. This is described in more detail in Hailey et. al.<sup>7</sup>

Instead of the usual flux versus energy curve for the sensitivity, we have plotted minimum detectable flux normalized at 50 keV versus spectral index. Because the objects of interest to us are characterized by a power law spectrum, we can immediately use the plot to determine whether we will be able to detect an object with a given flux and spectral index. The energy band of the observation has been optimized for each spectral index. Note that all the primary targets lie comfortably above detection threshold.

## 8. CONCLUSION

Arcminute imaging in the 30-200 keV range will allow important, new scientific observations of soft gamma-ray sources. Such observations require telescope components and a stabilized platform that can handle the arcminute pointing requirements. We have finished designing the critical components of the system to meet these requirements and construction of the experiment is underway. We expect to finish construction in December of 1990.

## 9. ACKNOWLEDGMENTS

We wish to acknowledge a grant from the Institute for Geophysics and Planetary Physics at LLNL and the University of California Campus-Laboratory Collaborative Research Program. This work was performed in part under the auspices of the U.S. Dept. of Energy by Lawrence Livermore National Laboratory under contract No. W-7405-ENG-48. FH is supported by a NASA GSRP grant.

## 10. REFERENCES

1. Dean, Nucl. Instr. Meth, 221, 265 1984.
2. J. E. Grindlay, M. R. Garcia, R. I. Burg and S. S. Murray, IEEE Trans. Nucl. Sci., NS-33, 750, 1986.
3. M.R. Garcia, J.E. Grindlay, R. Burg, S.S. Murray and J. Flanagan, IEEE Trans. Nucl. Sci. 33 (1), 735, 1986.
4. J. Braga, C. E. Covault and J. E. Grindlay, IEEE Trans. Nucl. Sci., NS-36,871, 1989.
5. C. J. Hailey, F. Harrison, J. H. Lupton and K. P. Ziock, Nucl. Instr. Meth., A276, 340, 1989.
6. F. Harrison, S. M. Kahn, C. J. Hailey, K. P. Ziock, M. Seiffert, P. M. Lubin, K. O. Ziock, (these proceedings).
7. J. Hailey, K. P. Ziock, F.A. Harrison, D. Liedahl, P. M. Lubin and M. Seiffert, Proc. of the SPIE, vol. 982, 16, 1988.
8. F. A. Primini, E. Basinska, S. K. Howe, F. Lang, A. M. Levine, R. Rothschild, W. A. Baity, D. E. Gruber, F. K. Knight, J. L. Matteson, S. M. Lea and G. A. Reichert, Ap. J., 243, L13, 1981.
9. A. W. Strong and G. F. Bignami, Ap. J., 274, 549, 1983.
10. S. M. Lea, G. Reichert, R. Mushotzky, W. A. Baity, D. E. Gruber, R Rothschild and F. A. Primini, Ap. J., 246, 369, 1981.
11. A. Bazzano, R. Fusco-Femiano, C. La Padula, V. F. Polcaro, P. Ubertini and R. K. Manchanda, Ap. J., 279, 515, 1984.
12. N. Kawai, E. E. Fenimore, J. Middleditch, R. G. Cruddace, G. G. Fritz, W.A. Snyder and M. P. Ulmer, Ap. J., 330, 130, 1988.

13. G. K. Skinner, A. P. Willmore, C. J. Eyles, D. Bertram, M. J. Church, P. K S. Harper, J. R.H. Herring, J. C. M. Peden, A. M. T. Pollock, T. J. Ponman and M. P. Watt, *Nature*, 330, 544, 1987.
14. W. R. Cook, D. M. Palmer, T. A. Prince, S. M. Schindler, C. H. Starr and E. C. Stone, IAU Symposium no. 136 on the Galactic Center, UCLA, in press.
15. P. M. Lubin, 1989, AIP Conf. Proc., submitted
16. A. Chingcuanco, Ph.D. thesis, University of California, Santa Barbara, 1989.

Table 1. Expected Performance GRATIS at 122 keV

Angular Resolution	1.7 arc minutes
Energy Resolution	~ 9%
Field of View	1.5° FWZI
Effective Area	346 cm <sup>2</sup>
Source Localization (10 $\sigma$ detection)	< 0.2 arc minutes
Energy Band	30 - 200 keV

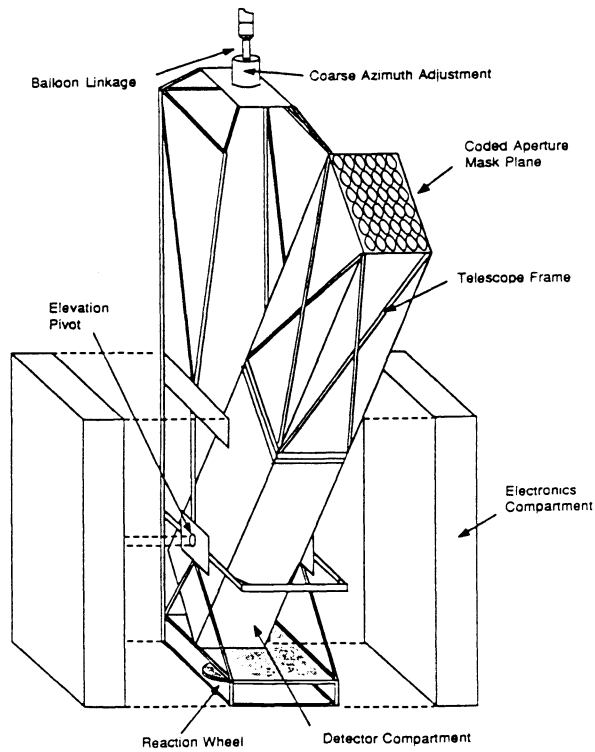


Figure 1. Schematic diagram of GRATIS balloon payload.

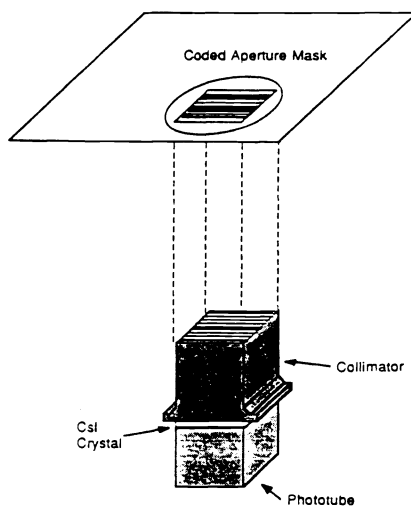


Figure 2. Diagram of small 1-D telescope.



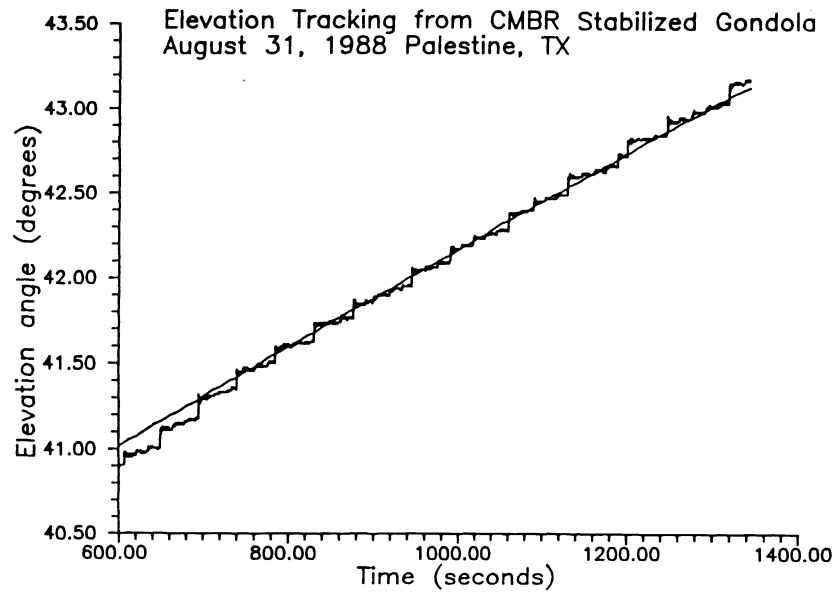


Figure 3a. In-flight elevation tracking of CMBR gondola. Straight line is desired elevation, stepped line is actual elevation.

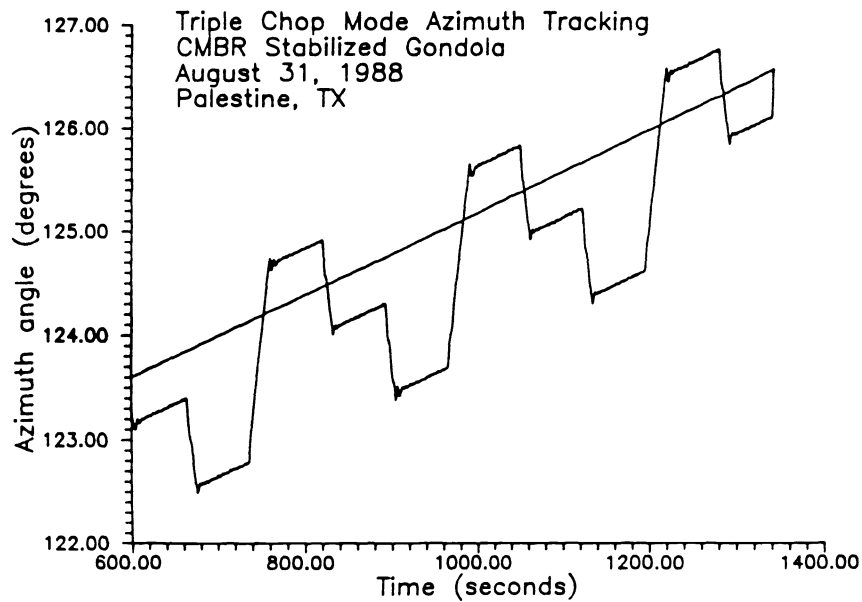


Figure 3b. In-flight triple chop azimuth tracking of CMBR gondola. Straight line is the azimuth of a point of constant right ascension and declination. The desired azimuth is a sequence of line segments parallel to the straight line but offset from it. The stepped line shown is the actual azimuth and is very close to the desired azimuth.

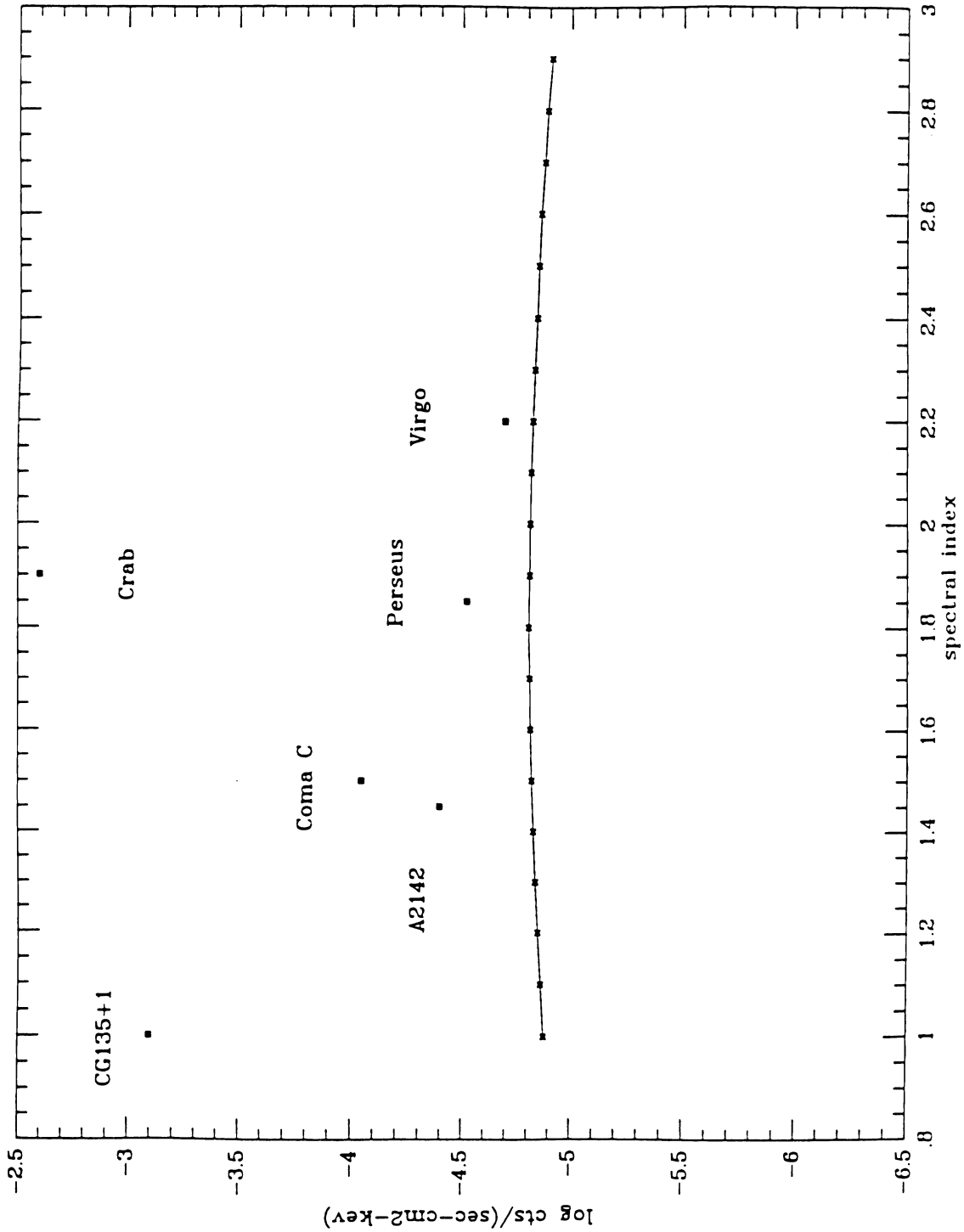


Figure 4. Minimum detectable flux at 50 keV vs spectral index for 5 sigma detection.